



**"Gheorghe Asachi" Technical University of Iasi, Romania**



---

## SPATIOTEMPORAL DISTRIBUTION AND PERIODICITY OF RAINFALL IN A TYPICAL ALLUVIAL PLAIN OF CHINA

Dan Huang<sup>1</sup>, Zaibin Liu<sup>1,2\*</sup>

<sup>1</sup>School of Environmental Science and Engineering, Chang'an University, Xi'an, 710054, Shaanxi, China

<sup>2</sup>Xi'an Research Institute Company of China Coal Technology and Engineering Group, Xi'an, 710054, Shaanxi, China

---

### Abstract

This paper aims to disclose the spatiotemporal distribution of rainfall in time domain or frequency domain. For this purpose, the rainfall data at seven stations in Hebei Plain since the 1960s were subjected to trend analysis by innovative trend analysis (ITA), Mann-Kendall (MK) test and linear regression and periodicity analysis by continuous wavelet transform (CWT). The results show that different rainfall intensities obeyed different trends on spatial and temporal scale. Firstly, on the annual scale, the rainfall decreased significantly at the confidence level of 10% at Raoyang, which lies in the centre of the study area, and heavy rainfall declined more significantly than the other four rainfall intensities. Secondly, on the seasonal scale, about half of the stations showed significant rainfall variations: summer rainfall is the major contributor to the decline in annual rainfall. Decreases of heavy rainfall in summer were recorded at Xingtai, Nangong and Huanghua, which may reduce the possibility of flood. Raoyang was highly sensitive to the rainfall with spring increase and summer/winter decrease, requiring more attention on winter drought. Thirdly, the rainfall in the middle of the study area has more significant period in 0.5-year and 0.83~1.17-year period scales. Finally, the results of the four methods agree well with rainfall variables. The research findings provide a valuable reference for water resources planning and drought or flood control.

**Key words:** continuous wavelet transform (CWT), innovative trend analysis (ITA), linear regression, Mann-Kendall (MK) test, periodicity analysis

*Received: September, 2018; Revised final: February, 2019; Accepted: March, 2019; Published in final edited form: May 2019*

---

### 1. Introduction

Since the early twentieth century, the global climate has undergone obvious changes (IPCC, 2007, 2014). In recent years, the climate change is characterized by the continued increase of greenhouse gas CS, which has greatly affected the groundwater level and rainfall (Badila, 2017; Balamurugan et al., 2018; Gotovsky et al., 2018; Huang et al., 2018; Liu et al., 2017; Ozdemir and Kaya, 2018; Pascale et al., 2016; Tu and Ma, 2018; Wright et al., 2015). Considering its significance to environment and human life, many scholars have explored the rainfall variation around the world and its impacts on human activities. For instance, Zhang et al. (2006)

investigated the rainfall and evaporation features over the past three decades in Hainan, China, shedding new light on water cycle balance and climate change features in China's tropical areas. Xiong and Xia (2009) and Russo et al. (2013) examined the effects of rainfall on mine inflow and put forward many protective measures for water resources. Focusing on the dry, terrace and coastal ecosystems in Bangladesh, Rahman et al. (2017) adopted the standardized precipitation index (SPI), diurnal temperature range (DTR) and rice productivity index (RPI) to measure the climate changes and their impacts on rice productivity in the said ecosystems, and recommended to introduce stress-tolerant and high temperature-resistant rice varieties requiring less irrigation water.

---

\* Author to whom all correspondence should be addressed: e-mail: zaibinliu@163.com; Phone: +86-13572198204

The traditional methods for the spatiotemporal distribution and periodicity of rainfall mainly include Mann-Kendall (MK) test, Spearman's Rho (SR) and continuous wavelet transform (CWT) (Grinsted et al., 2004; Kahya and Kalayci, 2004; Spearman, 1904). Rehman (2013) used the Mann-Kendall test and linear regression to study Long-term wind speed trends in the Kingdom of Saudi Arabia for the monthly and annual means and standard deviations. The magnitudes of the trends of increasing or decreasing wind speeds were derived from the Mann-Kendall rank statistics and the slope of the regression line by the least squares method. Coupling the MK test and linear regression, Caloiero et al. (2011) forecasted the annual and seasonal trends of rainfall in Calabria, Italy, revealing that the regional rainfall decreases annually and in autumn-winter but increases in summer. Based on the MK and SR, Shadmani et al. (2012) explored the annual, seasonal and monthly trends of reference evapotranspiration ( $ET_0$ ) at 11 sites in Iran from 1965 to 2005, and verified the agreement of the MK results and SR results on the trends for the  $ET_0$  series. Amirataee et al. (2016) applied the Mann-Kendall with considering the autocorrelation coefficients to analyze the trend of quantitative and qualitative changes in groundwater, in Iran. This article indicates that if the sample series are the time series, the autocorrelation coefficients are important. Compared to these traditional methods, the innovative trend analysis (ITA) can be implemented without restrictions on the length of time series, serial correlation and data distribution. To improve the trend analysis in time domain, Zekai Sen (2014) analyzed the rainfall trends in social, environmental, engineering, business and health variables using the ITA (Dabanlı et al., 2016; Markus et al., 2014). Haktanır and Citakoglu (2014) relied on the ITA to interpret the data series on annual maximum rainfall. Focusing on the rainfall records in Turkey, Oztopal and Sen (2017) employed the ITA by dividing the time series into three classes: low-, medium- and high-cluster.

Overall, these studies have shown that the rainfall or evaporation is partially controlled by inter-annual to multi-decadal climate variability. Targeting the rainfall variation in China, Xu (2016) applied the Morlet wavelet method to identify the periodic variation and cycle in rainfall of Tongchuan, Shaanxi Province. Zhang (2016) integrated the CWT, wavelet coherence analysis and global coherence coefficient to disclose the effects of monsoons and teleconnection

patterns on Niangziguan karst spring system in northern China.

Hebei Plain is the economic core area in the North China, water resources of the area become increasingly serious, and for exceeding exploitation of groundwater, cones of depression have formed (Shi et al., 2014; Zhang et al., 2011). There is densely inhabited district and has developed energy and heavy industry, water resources are shortage. Spring precipitation is little, spring drought and summer waterlogging are great threat to agricultural production (Gu, 2011). Groundwater, rivers and other water resources are mainly derived from rainfall. Therefore, disclosing the spatiotemporal distribution of rainfall in time domain or frequency domain in the study area is very necessary. This paper combines the ITA, MK and linear regression with the CWT to identify rainfall features and extremum distribution, compare the rainfall variation in different scales by the four methods, and determine the spatiotemporal distribution and periodicity of rainfall. The water shortage in the study area is caused by climate change and many other reasons (Wang et al., 2012). The research findings shed new light on water resource management in arid and semi-arid areas.

## 2. Study area

Located in the south of Hebei Province, Hebei Plain ( $36^{\circ}03' - 40^{\circ}15'N$ ,  $114^{\circ}05' - 119^{\circ}50'E$ ) is surrounded by the Taihang Mountains on the west and the Bohai Sea on the east. The whole plain is higher in the northeast and lower in the southeast. Most areas are less than 50m above sea level. Belonging to the warm temperate zone, the study area has a semi-arid continental monsoon climate. The study area was split into three geomorphic regions, namely, the sloping plain before the Taihang Mountains, the central flood plain and the eastern coastal plain. A total of 7 stations were selected in the study area (i.e. Xingtai, Nangong, Shijiazhuang, Raoyang, Huanghua, Baoding and Bazhou) with their data ID and data lengths shown in Table 1. The geographic information of these stations is presented in the digital elevation model (DEM) (30m) in Fig. 1. The monthly rainfall time series of the seven stations (1950–2015) were obtained from China Meteorological Data Network (<http://data.cma.cn>). The dataset of digital elevation is provided by Geospatial Data Cloud site, Computer Network Information Centre, Chinese Academy of Sciences (<http://www.gscloud.cn>).

**Table 1.** Basic statistical profile of seven stations

ID	station	Data period	Data length (year)	Elevation(m)
53798	Xingtai	1954-2015	62	73
54705	Nangong	1958-2015	58	28
53698	Shijiazhuang	1955-2015	61	82
54606	Raoyang	1957-2015	59	22
54624	Huanghua	1960-2015	56	7
54602	Baoding	1955-2015	61	25
54518	Bazhou	1957-2015	59	8

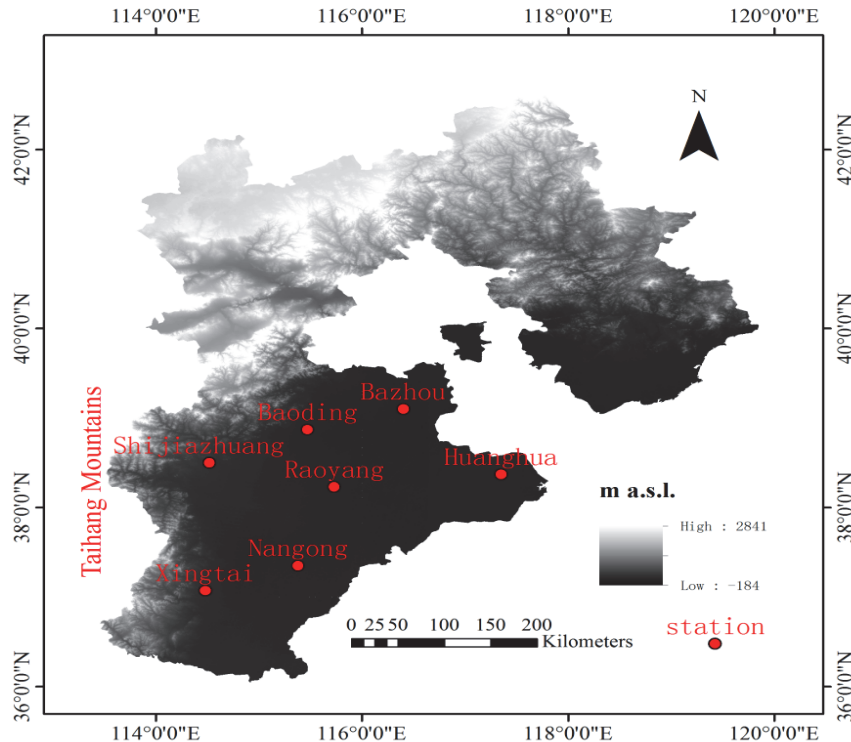


**Fig. 1.** Location map of the study area. The data set of digital elevation is provided by Geospatial Data Cloud site, Computer Network Information Center, Chinese Academy of Sciences (<http://www.gscloud.cn>)

### 3. Methodologies

#### 3.1. MK test

The MK test is a nonparametric trend test method recommended by the World Meteorological Organization (WMO). This test neither requires the sample to obey normal distribution nor face numerous outliers. Recent years has seen this method being widely adopted for the trend analysis on hydrologic, climate and abnormally distributed time series. The statistic  $S$  is expressed as (Eq. 1):

$$S = \sum_{i=1}^{n-1} \sum_{j=i+1}^n sgn(x_j - x_i) \quad (1)$$

where:  $x_i$  and  $x_j$  are data values at time  $i$  and  $j$  ( $j > i$ ), respectively;  $n$  is the number of the series, and  $sgn(x_j - x_i)$  is defined as (Eq. 2)

$$sgn(x_j - x_i) = \begin{cases} +1, & \text{if } (x_j - x_i) > 0 \\ 0, & \text{if } (x_j - x_i) = 0 \\ -1, & \text{if } (x_j - x_i) < 0 \end{cases} \quad (2)$$

Assuming that the data length  $n$  is longer than 10 and all the data are approximately normally distributed, the variance is given by (Eq. 3):

$$Var(S) = \frac{n(n-1)(2n+5) - \sum_{k=1}^m t_k(t_k-1)(2t_k+5)}{18} \quad (3)$$

where:  $m$  is the number of tied groups;  $t_k$  is the number of value in the  $m$ -th group. Thus, the standard normal test statistic  $Z$  can be calculated as (Eq. 4):

$$Z = \begin{cases} \frac{s-1}{\sqrt{Var(s)}}, & \text{if } S > 0 \\ 0, & \text{if } S = 0 \\ \frac{s+1}{\sqrt{Var(s)}}, & \text{if } S < 0 \end{cases} \quad (4)$$

If the absolute value of  $Z$  is greater than  $Z_{1-\alpha/2}$ , the null hypothesis must be rejected before identifying the monotonic trend in a two-tailed test at the significance level of  $\alpha$ . The trend is increasing if the value of  $Z$  is positive; otherwise, the trend is decreasing. Here, three significance levels are adopted below:

- \*\*\*trends at 0.01 level of significance;
- \*\*trends at 0.05 level of significance;
- \*trends at 0.1 level of significance.

#### 3.2. ITA

Unlike the MK or SR, the ITA does not require the independence or normal distribution of the data. The ITA has been widely used in to detect the trend of precipitation, evaporation and so on (Öztopal and Sen, 2017; Wu and Qian, 2017). By this method, the time series is divided into two or three equal subsamples and arranged in ascending order. To ensure the equal length of the subsamples, the first data will be ignored if the time series has an odd length. In a 2D Cartesian coordinate system, the first subsample is denoted as  $x_1$

and the others as  $y_i$ . Then, the identity line, or the 1:1 line, is drawn on the same system. The time series is trendless if the group of subseries is close to the 1:1 line and tolerable of an error of 5%~10%; the time series is increasing (decreasing) if the group is above (below) the 1:1 line.

The "D" indicator of the ITA was proposed by Wu and Qian for inland areas in continental monsoon climate zone. In their research, the rainfall intensity is categorized five groups according to percentiles: light (<10th percentile), low (10th~40th percentile), moderate (40th~60th percentile), high (60th~90th percentile) and heavy (>90th percentile) (Wu and Qian, 2017). The algorithm proposed by Wu and Qian (2017) was adopted for our study area which has a semi-arid continental monsoon climate (Eq. 5).

$$D = \frac{1}{n} \sum_{i=1}^n \frac{10(y_i - x_i)}{x} \quad (5)$$

### 3.3. CWT

Continuous wavelet transform is an effective tool for time series analysis, such as analysis of precipitation and runoff in karst watershed, prediction of ground water level and discussion of relationship between climate patterns and water level (Adamowski and Chan, 2011; Kuss and Gurdak, 2014; Labat et al., 1999). In this study, we choose Morlet wavelet as mother wavelet, because it is a zero mean function and symmetrical in both frequency and time domains. The Morlet wavelet is defined as (Eq. 6):

$$\varphi_0(\mu) = \pi^{-\frac{1}{4}} e^{i\omega_0\mu} e^{-\frac{1}{2}\mu^2} \quad (6)$$

where  $\omega_0$  is the dimensionless frequency;  $\mu$  is the dimensionless time. The dimensionless frequency is usually set to 6.

For a time series ( $x_t = 1, \dots, N$ ) with uniform time step  $\delta t$ , the CWT is defined as the convolution of  $x_t$  with the scaled and transformed wavelet (Eq. 7).

$$W_x(a, \tau) = \sqrt{\frac{\delta_t}{a}} \sum_{t=1}^N x_t \varphi_0^* \left[ \left( t - \tau \right) \frac{\delta_t}{a} \right] \quad (7)$$

where  $a$  is the scale expansion factor;  $\tau$  is the time shift factor;  $t$  is the dimensionless time. The  $W_x(a, \tau)$  can project the time series into a 2D time-frequency space.

However, the CWT has an edge effect due to the not completely localized in time. The cone of influence (COI) is designed to solve the problem. The wavelet power can be assessed by a given background power spectrum ( $P_k$ ), which is the 5% significance level against the red noise generated from a first order autoregressive (AR1) process.  $P_k$  expressed as (Eq. 8):

$$P_k = \frac{1 - \alpha^2}{|1 - \alpha e^{-2i\pi k}|^2} \quad (8)$$

where  $\alpha$  is the correlation coefficient of the AR1;  $k$  is the Fourier frequency index.

## 4. Results and discussions

### 4.1. Rainfall features

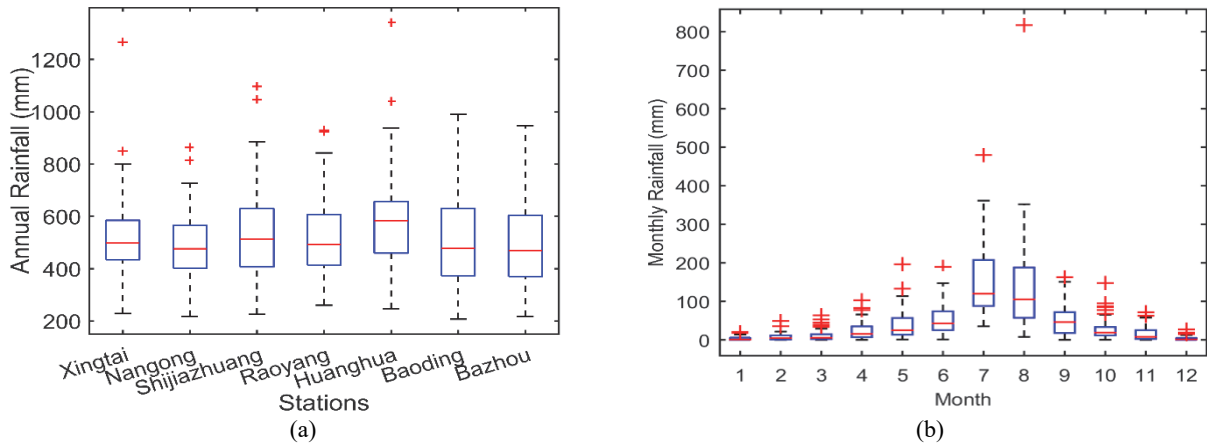
In boxplot diagrams, every boxplot consists of one box and two segments controlled by the maximum, minimum, the 25th, 50th and 75th percentiles, extremums and outliers. As shown in Fig. 2(a), the rainfall varied only slightly from south to north and from west to east, and the outliers were observed on the upper side of alluvial plain like Xingtai and Nangong.

The monthly rainfall of Xingtai is detailed in Fig. 2(b), because the station lies at the southernmost end and has a similar variability to other stations. It can be seen that the rainfall concentrated in June, July and August, taking up about 70% of the annual rainfall, while little rain occurred in spring. As a result, spring drought and summer flood have great impact on agriculture.

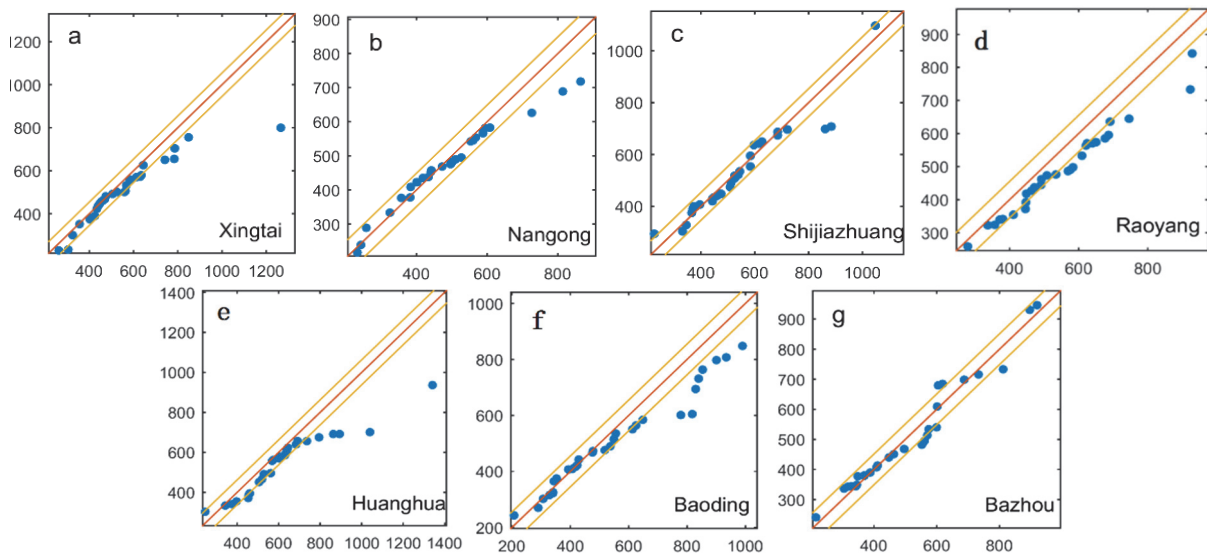
### 4.2. Annual trends

Table 2 sums up the annual rainfall trends disclosed by the ITA, MK and linear regression. Note that the results of the three methods are recorded as the following parameters: the slope of linear regression  $b$ , which reflects the increase/decrease rate, the statistics  $z$  are selected with the mark '\*' at the 90%, 95% or 99% for two-tailed confidence levels, and the D indicator of the ITA, with 10th, 40th, 60th and 90th percentiles as the critical points. Table 2 demonstrates that the rainfall at Raoyang, located in the center of the study area, exhibited a decreasing trend at the 90% significant level, and its decreasing rate surpassed -2mm/year. Besides, the D values varied with the rainfall intensities. With the increase intensity of the rainfall, the D values decrease, in other words, the more intensity the rainfall has, the more obvious the trend is. The rainfall firstly plunged deeply and then slightly across all stations, as evidenced by the results on Shijiazhuang (sloping plain before the Taihang Mountains), Raoyang (central flood plain) and Huanghua (eastern coastal plain). The rainfall variation directly bears on the karst action in northern China, and the distribution and enrichment of karst groundwater depend heavily on the climate and meteoric water line (Wang et al., 2007). The rainfall is in general decreasing in the region, it may be the reason why the karst water resource decreased from 1980s in the Karst area in northern China.

According to the ITA results of the seven stations in Fig. 3, the points at most stations fell below the 1:1 line, indicating a downward trend in rainfall. Comparing the data of each station, it is clear that different rainfall intensities had different trends.



**Fig. 2.** Boxplots of (a) the annual rainfall of the 7 stations, and (b) monthly rainfall of Xingtai



**Fig. 3.** The ITA scatter diagram of annual rainfall (a-g)

**Table 2.** Annual rainfall trends disclosed by the ITA (D), MK (Z) and linear regression (b)

Station	<i>b</i>	<i>Z</i>	D					
			Annual	Light	Low	Moderate	High	Heavy
Xingtai	-1.78	-1.00	-0.89	-0.61	-0.26	-0.26	-0.83	-3.54
Nangong	-0.89	-0.72	-0.32	0.06	0.29	-0.14	-0.39	-2.53
Shijiazhuang	-0.98	-0.42	-0.22	0.15	0.04	-0.38	0.05	-1.80
Raoyang	-2.02*	-1.74*	-1.13	-0.41	-0.81	-1.03	-1.33	-2.29
Huanghua	-2.75*	-1.22	-1.21	0.08	-0.94	-0.43	-1.02	-5.06
Baoding	-2.21	-1.15	-0.86	0.06	0.01	-0.38	-1.88	-2.25
Bazhou	-0.68	-0.22	-0.09	0.53	0.16	-0.60	-0.17	-0.11

For Raoyang (Fig. 3(d)), light and low rainfalls decreased slightly, while moderate, high and heavy rainfalls exhibited a strong declining trend: the rainfall above 700mm/year was reduced by over 10%. For most stations (Fig. 3a-c and 3e, light, low, moderate and high rainfalls decreased slightly, while heavy rainfall decreased dramatically. For Baoding (Fig. 3f), no significant trend was observed at the rainfall below 600mm/year, but abrupt decrease occurred after the rainfall exceeded that level. For Bazhou (Fig. 3g), all the points fell between the -10% line and the +10% line, suggesting no significant trend for all the rainfall intensities. In recent decades, most stations recorded

weak or obvious decline in rainfall, a sign of the arid trend in Hebei Plain.

#### 4.3. Seasonal trends

The results of rainfall trends by the ITA, MK and linear regression are listed in Table 3. From section 4.1, we know spring drought and summer flood phenomenon appeared in the study area, besides the lack of space, the table only presents the results in spring and summer. For spring time series, significant increases ( $\alpha=0.05$  and  $0.1$ ) were observed at four stations (Nangong, Raoyang, Huanghua and Bazhou),

accounting for more than half of observation stations. For summer time series, significant decreases ( $\alpha=0.05$  and 0.1) existed at four stations (Nangong, Raoyang, Huanghua and Baoding). For autumn time series, significant increase ( $\alpha=0.05$ ) occurred only at one station (Bazhou). For winter time series, significant increase ( $\alpha=0.05$ ) happened at one station (Raoyang).

Comparing the data on different stations, it is learned that Raoyang and Nangong were more sensitive than others. Nangong underwent significant rainfall variations in two seasons (i.e. the increase in spring and the decrease in summer), that can explain why no significant trends exist in annual at Nangong station. For Raoyang, the rainfall fluctuated violently in three seasons, including the increase in spring and the decline in summer and winter. With the spring increase, the summer and winter decreases, which contribute to the annual decline at the station, seem more drastic. In other words, this station is less likely to suffer from drought in spring than summer or winter.

Rainfall has an important influence on agriculture, water supply and karst groundwater resources. According to China Meteorological Data Network, ten severe droughts hit Hebei Province from 1950 to 1999, most of which occurred in summer and autumn. In northern China, summer is the critical period for corn growth while winter for winter wheat. Thus, it is necessary to cultivate drought tolerant strains.

Considering the sharp decline in summer, the ITA results on summer rainfall are shown in Fig.4 below. Despite the unobvious variation for most rainfall intensities, Fig. 4(a-b) and 4(e) presents noticeable changes in heavy rainfall, that is, greater-than-10% decreases were observed at Xingtai, Nangong and Huanghua. The marked decreases mostly took place on the southern and eastern edges of the study area. It is worthy of mentioning that, although the heavy rainfall dropped sharply, the overall trend of summer rainfall was stable at Xingtai.

Thus, it is useful to study the extrema like the heavy rainfall. The results show that the rainstorms may reduce in summer, which helps to mitigate the flood.

#### 4.4. Periodic distribution analysis

To quantify the oscillating periodic rainfall variations, CWT was conducted. The features of rainfall series for all stations were extracted by the CWT. For the lack of space, only the stations (Shijiazhuang, Raoyang and Huanghua) in the north-south and east-west direction of alluvial plain are presented in Fig. 5, where warm and cool colors stand for the peaks and valleys of energy density, respectively. The energy density reflects the locality and dynamics of time-frequency transform of the dominant fluctuations. The thick black contour expresses the 5% significance level against the red noise; the thin black contour refers to the COI; the lighter shade under the COI is negligible as the effect of edge effect.

The CWT spectrograms indicate that the seven time series shared common features in the wavelet power. From Fig. 5, there is a main oscillation period of 0.77~1.16a and a second oscillation period of 0.5a. In the low-frequency part, the energy density was discontinuous in the 0.83~1.17-year periodic scale, but almost all the years have significant frequency-domain periodic features and pass the 95% confidence level test. In the high-frequency part, the energy density was discontinuous in the 0.5-year periodic scale, with only a few years passing the 95% confidence level test. Hence, in the 0.5-year periodic scale, there was no significant periodic features for the rainfall. In the 0.5-year period scale, the spectrograms differed from each other in the north-south or east-west direction. The number of years passing the 95% confidence level test increased from south (Xingtai) to north (Bazhou) and from west (Shijiazhuang) to east (Huanghua).

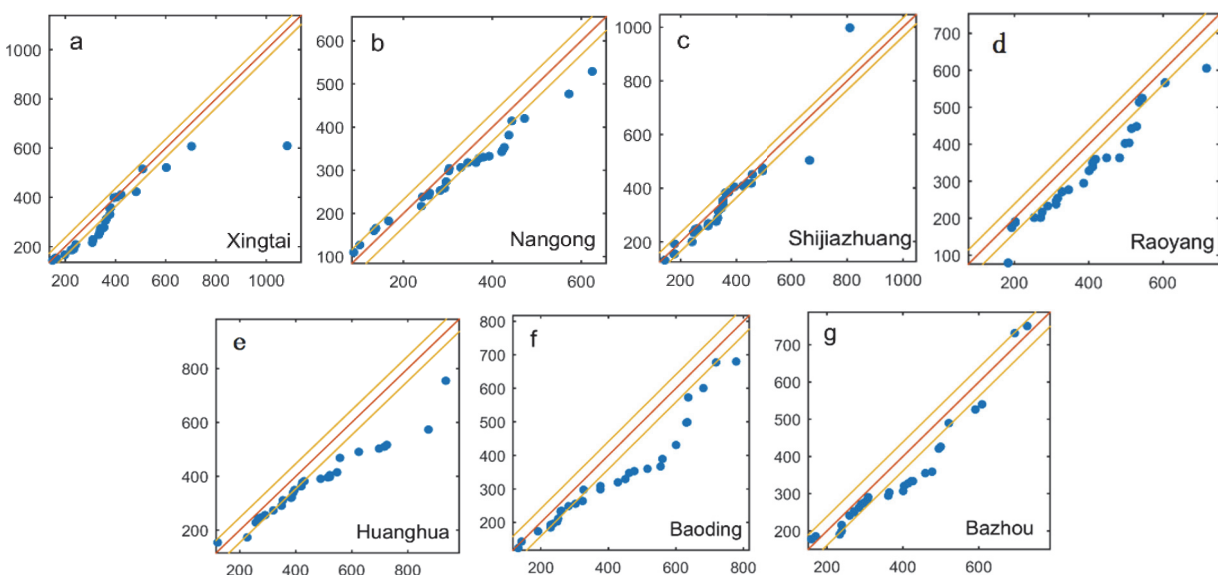
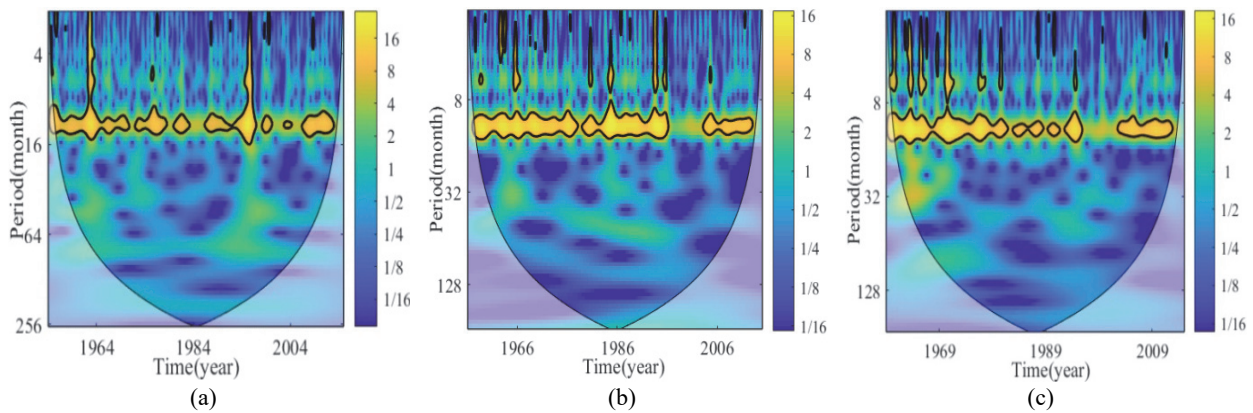


Fig. 4. ITA results of the seven stations



**Fig. 5.** The wavelet transforms spectrograms of precipitation at different stations. Figures of CWT for Shijiazhuang, Raoyang and Huanghua are shown from left to right: (a), (b), (c)

**Table 3.** Seasonal rainfall trends disclosed by the ITA (D), MK (Z) and linear regression (b)

<b>Station</b>	<b>Spring</b>			<b>Summer</b>		
	<b>b</b>	<b>Z</b>	<b>D</b>	<b>b</b>	<b>Z</b>	<b>D</b>
Xingtai	0.25	1.14	2.38	-2.00*	-1.35	-1.62
Nangong	0.59*	2.35**	3.57	-1.52*	-1.95*	-0.91
Shijiazhuang	0.00	0.88	0.32	-1.07	-0.96	-0.41
Raoyang	0.37	1.87*	1.83	-2.20**	-2.18**	-1.65
Huanghua	0.41	1.82*	0.67	-3.42**	-2.04**	-1.98
Baoding	0.25	1.33	2.26	-2.78**	-2.06**	-1.87
Bazhou	0.32	1.86*	2.68	-1.68	-1.26	-1.14

In the 0.83~1.17 year period scale, the number of years passing the 95% confidence level test in Raoyang and Nangong were greater than that of others stations. This means the periodic rainfall is more significant in the center of the study area than the other areas. Further research is needed to see if location is the only reason for these significant periods

## 5. Conclusions

Through the MK, ITA and linear regression on the rainfall data recorded at seven stations in our study area, the following conclusions were put forward:

(1) Across the study period, only one station, Raoyang, showed a significant trend in annual rainfall, that is, a decline faster than -2mm/year. For ITA method, the D values of different rainfall categories sometimes opposite, moreover usually do not equal those of the overall rainfall. With the increase of rainfall intensity, the decreasing trend is more obvious.

(2) The stations exhibited significant rainfall variations through the four seasons. For some stations, the rainfall may fluctuate violently in spring but slightly in summer. Among the seven stations, four stations underwent significant variations in spring, four in summer, one in autumn, and one in winter. The general trends are increases in spring and autumn and decreases in summer and winter. The summer decline is the major contributor to the decrease of annual rainfall. Raoyang had the most pronounced seasonal rainfall variations, with significant changes observed in all four seasons. In summer, the heavy rainfall showed marked decreases at Xingtai, Nangong and

Huanghua. From the west to the east, the decrease amplitude firstly narrowed and then widened.

(3) The results of trend analysis (MK, ITA and linear regression) agree well with each other, and in study area, rainfall dynamics have a main oscillation period of 0.77~1.16a.exa.

The above results lay a solid basis for water resources planning and drought or flood control. In future, the rainfalls of different stations in different climate zones will be investigated to verify if the ITA indicator D could be used to evaluate different dimension parameters with different orders of magnitudes, and to identify the causes to the periodic difference of rainfall from the center to the edge of the study area.

## References

- Adamowski J., Chan H.F., (2011), A wavelet neural network conjunction model for groundwater level forecasting. *Journal of Hydrology (Amsterdam)*, **407**, 28-40.
- Amirataee B., Zeinalzadeh K., (2016), Trends analysis of quantitative and qualitative changes in groundwater with considering the autocorrelation coefficients in west of Lake Urmia, Iran, *Environmental Earth Sciences*, **75**, DOI 10.1007/s12665-015-4917-2.
- Badila A.S., (2017), Impacts of production and storing of organic manure over the quality of groundwater in the basin of Geru River from Galaty County, *Environmental Engineering and Management Journal*, **16**, 653-668.
- Balamurugan T., Karunamoorthy L., Arunkumar N., Santhosh D., (2018), Optimization of Inventory Routing Problem to Minimize Carbon Dioxide Emission, *International Journal of Simulation Modelling*, **17**, 42-54

- Caloiero T., Coscarelli R., Ferrari E., (2011), Trend detection of annual and seasonal rainfall in Calabria (Southern Italy), *International Journal of Climatology*, **31**, 44-56.
- Dabanlı I., Sen Z., Yelegen M.Ö., Sisman E., Selek B., Güçlü Y.S., (2016), Trend Assessment by the Innovative-Sen Method, *Water Resources Management*, **30**, 5193-5203.
- Gotovsky M., Gotovsky A., Mikhailov V., Kolpakov S., Lychakov V., Sukhorukov Y., (2018), Formic acid cycle as partial alternative to Allam cycle less expensive and simpler, *TECNICA ITALIANA-Italian Journal of Engineering Science*, **62**, 49-54.
- Grinsted A., Moore J.C., Jevrejeva S., (2004), Application of the cross wavelet transform and wavelet coherence to geophysical time series, *Nonlinear Processes in Geophysics*, **11**, 561-566.
- Gu H., (2011), *Study on topographic geochemistry feature of the Hebei Plain*, Dissertation, Shijiazhuang University of Economics, China.
- Haktanır T., Citakoglu H., (2014), Trend, independence, stationarity, and homogeneity tests on maximum rainfall series of standard durations recorded in Turkey, *Journal of Hydrologic Engineering*, **19**, 171-195.
- Huang Z.H., Zhu Z.Q., Zhou Z.H., (2018), Harmful gas reduction through synthesis of epoxy resin aqueous dispersion, *Revue des Composites et des Matériaux Avancés*, **28**, 529-538.
- Intergovernmental Panel on Climate Change (IPCC), (2007), Climate change 2007: Impacts, Adaptation, and Vulnerability, Contribution of Working Group II to the Fourth Assessment Report of the Intergovernmental Panel on Climate Change, Cambridge University Press: Cambridge, UK.
- Intergovernmental Panel on Climate Change (IPCC), (2014), Climate Change 2014: Impacts, Adaptation, and Vulnerability, Contribution of Working Group II to the Fifth Assessment Report of the Intergovernmental Panel on Climate Change, Cambridge University Press: Cambridge, UK.
- Kahya E., Kalayci S., (2004), Trend analysis of streamflow in Turkey, *Journal of Hydrology*, **289**, 128-144.
- Kuss A.J.M., Gurdak J.J., (2014), Groundwater level response in U.S. principal aquifers to ENSO, NAO, PDO and AMO, *Journal of Hydrology*, **519**, 1939-1952.
- Labat D., Ababou R., Mangin A., (1999), Wavelet analysis in karstic hydrology. 2nd part: rainfall-runoff cross-wavelet analysis. 2nd part: rainfall-runoff cross-wavelet analysis, *Comptes Rendus de L'académie des Sciences*, **329**, 881-887.
- Liu Y., Tian Y., Chen M., (2017), Research on the prediction of carbon emission based on the chaos theory and neural network, *International Journal Bioautomation*, **21**, 339-348.
- Markus M., Demissie M., Short M.B., (2014), Sensitivity analysis of annual nitrate loads and the corresponding trends in the lower Illinois River, *Journal of Hydrologic Engineering*, **19**, 533-543.
- Ozdemir O., Kaya A., (2018), K-medoids and fuzzy C-means algorithms for clustering CO<sub>2</sub> emissions of Turkey and other OECD countries, *Applied Ecology and Environmental Research*, **16**, 2513-2526.
- Öztopal A., Sen Z., (2017), Innovative trend methodology applications to precipitation records in Turkey, *Water Resources Management*, **31**, 727-737.
- Pascale S., Lucarini V., Feng X., (2016), Projected changes of rainfall seasonality and dry spells in a high greenhouse gas emissions scenario, *Climate Dynamics*, **46**, 1331-1350.
- Rahman M.A., Kang S.C., Nagabhatla N., (2017), Impacts of temperature and rainfall variation on rice productivity in major ecosystems of Bangladesh, *Agriculture & Food Security*, **6**, DOI 10.1186/s40066-017-0089-5.
- Rehman S., (2013), Long-term wind speed analysis and detection of its trends using Mann-Kendall test and linear regression method, *Arabian Journal for Science and Engineering*, **38**, 421-437.
- Russo S.L., Gnani L., Peila D., (2013), Rough evaluation of the water-inflow discharge in abandoned mining tunnels using a simplified water balance model: the case of the Cogne iron mine (Aosta Valley, NW Italy), *Environmental Earth Sciences*, **70**, 2753-2765.
- Şen Z., (2014), Trend Identification Simulation and Application, *Journal of Hydrologic Engineering*, **19**, 635-642.
- Shadmani M., Marofi S., Roknian M., (2012), Trend analysis in reference evapotranspiration using Mann-Kendall and Spearman's Rho tests in arid regions of Iran, *Water Resources Management*, **26**, 211-224.
- Shi J.S., Li G.M., Liang X., (2014), Evolution mechanism and control of groundwater in the North China Plain, *Acta Geoscientica Sinica*, **35**, 527-534.
- Spearman C., (1904), The proof and measurement of association between two things, *American Journal of Psychology*, **15**, 72-101.
- Tu J.Z., Ma D.L., (2018), A spatial economics perspective on convergence research of carbon emissions performance in China, *International Journal of Heat and Technology*, **36**, 962-972.
- Wang Y.J., Liu J.M., Wang P.X., (2007), Prediction of drought occurrence based on the Standardized Precipitation Index and the Markov Chain Model with weights, *Agricultural Research in the Arid Areas*, **25**, 198-202.
- Wang W.T., Liang Y.P., Wang Z.H., Zhao C.H., (2012), Characteristics of climate change in northern China and its effect on groundwater in karst areas, *Hydrogeology and Engineering Geology*, **39**, 6-10.
- Wright I.A., McCarthy B., Belmer N., (2015), Subsidence from an underground coal mine and mine wastewater discharge causing water pollution and degradation of aquatic ecosystems, *Water Air & Soil Pollution*, **226**, 1-14.
- Wu H., Qian H., (2017), Innovative trend analysis of annual and seasonal rainfall and extreme values in Shaanxi, China, since the 1950s, *International Journal of Climatology*, **37**, 2582-2592.
- Xiong B., Xia K.Q., (2009), Time series analysis on mine inrush water quantity in Yutianbao Mine, *Coal Science and Technology*, **37**, 95-98.
- Xu P.P., Wang H.K., Qian H., Li Y.B., (2016), Analysis of precipitation variation and trend forecast in Tongchuan, *Journal of Water Resources & Water Engineering*, **27**, 82-86.
- Zhang L.M., Wei Z.Y., Qi Z.P., (2006), Characteristics of rainfall and evaporation of different region in recent 30 years in Hainan Province, *Chinese Agricultural Science Bulletin*, **22**, 403-407.
- Zhang G.H., Lian Y.L., Liu C.H., (2011), Situation and origin of water resources in short supply in North China plain, *Journal of Earth Sciences and Environment*, **33**, 172-176.
- Zhang J., Hao Y., Hu B.X., (2016), The effects of monsoons and climate teleconnections on the Niangziguang Karst Spring discharge in North China, *Climate Dynamics*, **48**, 1-18.